

QUANTUM CHEMICAL STUDY ON THE SOLVATION  
OF LITHIUM CHLORIDE IN DIMETHYL AND DIETHYL SULFONES

A. S. MKHITARYAN, Z. K. PAPANYAN, L. S. GABRIELYAN\*

*Chair of Physical and Colloids Chemistry YSU, Armenia*

LiCl–dimethyl sulfone and LiCl–diethyl sulfone systems have been investigated by restricted Hartree-Fock (RHF/6-311++G(d, p)) computations in order to establish the structural and spectral parameters of solute–solvent systems. The calculations show the existence of two stable LiCl–sulfone (1:1) structures and one transition state. It was shown that sensitivity of the CH and SO stretching vibrations to the interaction between LiCl and sulfone strongly depends on the structure of the complex, and the difference in their properties is explained in the frame of vibrational Stark effect, rather than by specific solute-solvent interactions only. Results are compared to the solid state experimental spectra.

**Keywords:** sulfone, lithium chloride, *ab initio* calculations, IR spectra, Stark effect.

**Introduction.** In the recent years lithium-ion batteries have been widely applied for portable electronic devices such as cellular phones and personal computers [1]. Solutions of lithium salts in various aprotic dipolar solvents are considered as a media for transferring of charges between two electrodes. Among electrolytes for lithium-ion batteries, sulfone-based electrolytes are especially interesting, because of their high resistivity to electrode materials and ability to ensure high speed of electrode process [2, 3]. The unique properties of sulfones such as large dipole moments (4.44 D for dimethyl sulfone (DMSO<sub>2</sub>)) and especially dielectric constants (47.39 for DMSO<sub>2</sub>) arise from inhomogeneous distribution of the electrostatic potential on the surface of these molecules [4]. The number of experimental and theoretical studies such as phase diagrams, conductivity, viscosity and oxidation potential for the lithium salt solutions in sulfone containing solvents has been reported [2, 5–9]. Theoretical methods such as *ab initio* methodologies and molecular dynamics techniques provide the understanding of the ion-solvent interactions at the microscopic level. The present work was undertaken to study the local structures of LiCl in DMSO<sub>2</sub> and diethyl sulfone (DESO<sub>2</sub>) by performing the quantum chemical computations. In this study the optimized geometries, charge distribution and vibrational spectra using restricted Hartree–Fock method with various basis sets have been calculated. The transition state structures have been also determined. Besides that the experimental vibrational analysis of LiCl–DMSO<sub>2</sub> has been performed.

---

\* E-mail: [lgabriel@ysu.am](mailto:lgabriel@ysu.am)

DMSO2 (98%, “Sigma Aldrich”) and lithium chloride (anhydrous 98%, “Fluka”) were used without further purification. Since DMSO2 is a solid at room temperature, to prepare the LiCl solution the intimate mixture of two powders was heated to the melting point of sulfone (~110°C) in a sealed container and the completeness of dissolution was monitored visually. All solutions were prepared gravimetrically; it was found that at least 4 mol of DMSO2 are needed to completely dissolve 1 mol of LiCl. The melt was cooled to room temperature and solid obtained was used in FTIR measurement. No additional work was done to investigate the crystalline structure/exact composition of obtained solid, we assume that it should contain possible solvated ionic species either as a separate phase or a solid solution, as well as unreacted reagents.

The FTIR spectra were recorded using Nicolet/FTIR NEXUS spectrometer equipped with a DTGS detector, a CsI beam splitter and globar source. The infrared spectra of pure polycrystalline solid DMSO2 and 1 : 4 molar ratio LiCl : DMSO2 solid solution were obtained with ATR attachment in the 4000–600  $\text{cm}^{-1}$  region at room temperature. The ATR cell is made of trapezoidal ZnSe crystal with an incident angle of 45° and 12 reflections. Data were collected with a resolution of 4  $\text{cm}^{-1}$  and 32 parallel scans.

The molecular geometry optimizations, energy and fundamental vibration frequency calculations have been carried out using Gaussian 09 program package [10]. The molecular structure optimization of isolated DMSO2, DESO2 molecules and of the LiCl–sulfone (1:1) complexes in their ground states in the gas phase were performed using restricted Hartree–Fock (RHF) method combined with 6-311++G(d, p) extended basis set including polarization and diffuse functions. Energy minima were confirmed by the absence of imaginary vibration frequency. The transition state structures with one imaginary mode were also determined. The assignments of the calculated frequencies were done by GaussView 5.0 program, which gives a visual presentation of the vibrational modes [11].

### Results and Discussion.

**Dimethyl and Diethyl Sulfones.** In the first step of calculations, geometry optimizations on isolated DMSO2 and DESO2 molecules were performed by using RHF/6-311++G(d, p) basis set to determine the most stable conformers. The optimized structures and atomic numbering scheme of DMSO2 and DESO2 are shown in Fig. 1.

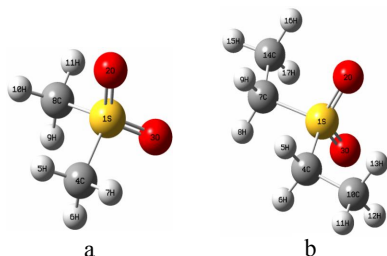


Fig. 1. Optimized structures of DMSO2 (a) and DESO2 (b).

The full output of calculated structural parameters, bond lengths, bond angles and dihedral angles is listed in Tab. 1.

Comparison of the obtained optimized structure of DMSO2 with the experimentally determined geometry (given in brackets [12]) shows good agreement and indicates that 6-311++G(d, p) basis set describes the systems under study quite well. In contrast to DMSO2 there is no experimental data reported in the literature for DESO2 molecule. The S–O, S–C, C–H bonds lengths in DESO2 are relatively longer than in DMSO2, but bond angles OSO and CSC are smaller. This difference can be explained by the larger electron-donating effect of ethyl group in

comparison with methyl group, given the fact that the sulfur–oxygen linkages are not double bonds, as is widely believed, but are rather coordinate covalent single  $S^+ \rightarrow O^-$  bonds [4]. In both molecules the configuration of sulfur is distorted tetrahedral. The global minimum energy obtained by RHF/6-311++G(d, p) basis set for DMSO2 and DESO2 are calculated as  $-626.4781319$  and  $-704.5695735$  Hartree respectively.

Table 1

The calculated main structural parameters for DMSO2 and DESO2 at RHF/6-311++G(d, p) level

Parameters *	DMSO2	Parameters	DESO2
r(S1–O3)	1.4314 (1.431 [12])	r(S1O3)	1.4351
r(S1–O2)	1.4314 (1.431 [12])	r(S1O2)	1.4351
r(S1–C4)	1.7741 (1.777 [12])	r(S1C4)	1.7856
r(S1–C8)	1.7741 (1.777 [12])	r(S1C7)	1.7856
r(C4–H5)	1.0814	r(C4C10)	1.5273
r(C4–H6)	1.0814	r(C7C14)	1.5273
r(C4–H7)	1.0822	r(C4H5)	1.0836
r(C8–H9)	1.0814	r(C7H9)	1.0836
r(C8–H10)	1.0814	r(C10H11)	1.0845
r(C8–H11)	1.0822	r(C10H12)	1.0829
$\angle(O2S1O3)$	119.71 (121.0 [12])	$\angle(O2S1O3)$	119.01
$\angle(C8S1C4)$	104.61 (103.1 [12])	$\angle(C7S1C4)$	104.22
$\angle(C8S1O3)$	107.88	$\angle(C4S1O3)$	108.16
$\angle(H5C4H6)$	111.66	$\angle(H5C4H6)$	109.41
$\angle(H9C8H11)$	110.04	$\angle(H6C4H10)$	111.49
$\phi(C4S1C8H11)$	180.0	$\phi(C4S1C7C14)$	180.0
$\phi(H5C4S1O2)$	53.3	$\phi(C14C7S1O2)$	65.1
Energy, Hartree	$-626.4781319$	Energy, Hartree	$-704.56957355$
Dipole Moment, D	5.41	Dipole Moment, D	5.13
Charge		Charge	
S1	0.548122	S1	0.476944
O2	$-0.327768$	O2	$-0.302611$
O3	$-0.327768$	O3	$-0.302611$

\* Bond lengths in Å, bond angles and dihedral angles in °, 1 Hartree = 2625.5 kJ/mol.

**LiCl–DMSO2 and LiCl–DESO2 Systems.** The potential energy surface of the 1:1 LiCl–DMSO2 complex was scanned by RHF calculations and produced two minimum energy structures, which are illustrated in Fig. 2, a and b. The absence of imaginary frequencies in each of the resulting structures was used to verify that they correspond to true minima on the potential energy surface. A similar analysis was performed for LiCl–DESO2 system, although this is a more complex system, and for pure DESO2 very few data are available in literature.

In the first structure (Fig. 2, a and Fig. 3, a) the coordination of lithium ion with sulfone molecules occurs through one oxygen atom (monodentate). In the second structure bidentate coordination of lithium ion is detected (Fig. 2, b and Fig. 3, b). Interestingly, same coordination types and similar geometries were reported for DMSO2–Li<sup>+</sup> complex cation while measuring lithium-cation and proton affinities of sulfoxides and sulfones [13]. Additionally, lithium-oxygen linkage was detected by IR spectroscopy in alkali salts–dialkyl sulfoxides solutions by appearance of a new low frequency mode at  $429\text{ cm}^{-1}$  [14], whereas our calculations of LiCl–DMSO2 structures reveal new peaks under 413,  $627\text{ cm}^{-1}$  for I structure (O–Li–Cl sym.,

asym. stretches) and  $540\text{ cm}^{-1}$  for II structure (Li–O<sub>2</sub> stretch) proving Li<sup>+</sup> coordination by oxygen atoms.

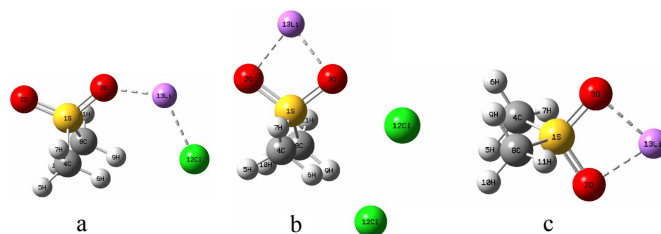


Fig. 2. Optimized structures of 1:1 LiCl–DMSO<sub>2</sub> stable complexes: I structure (a), II structure (b) and transition state structure (c).

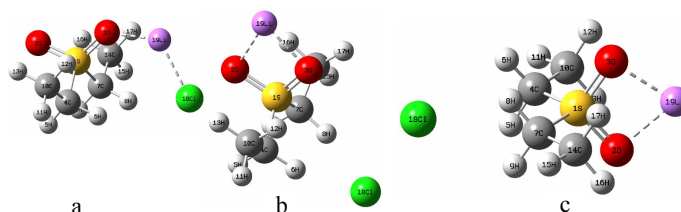


Fig. 3. Optimized structures of 1:1 LiCl–DMSO<sub>2</sub> stable complexes: I structure (a), II structure (b) and transition state structure (c).

Table 2

Some optimized structural parameters for 1:1 LiCl–DMSO<sub>2</sub> stable complexes and transition state at RHF/6-311++G(d, p) level

Parameters	LiCl–DMSO <sub>2</sub> (I structure)	LiCl–DMSO <sub>2</sub> (II structure)	LiCl–DMSO <sub>2</sub> (transition state)
r(S1–O3)	1.4584	1.4659	1.4730
r(S1–O2)	1.4267	1.4761	1.4730
r(S1–C4)	1.7695	1.7600	1.7609
r(S1–C8)	1.7695	1.7600	1.7609
r(C4–H5)	1.0815	1.0821	1.0793
r(C4–H6)	1.0818	1.0880	1.0793
r(C4–H7)	1.0824	1.0823	1.0834
r(C8–H9)	1.0818	1.0880	1.0793
r(Li13–O2)		1.9338	1.9226
r(Li13–O3)	1.8413	1.9086	1.9226
r(Li13–Cl12)	2.1178		
r(Cl12–H9)	2.9686	2.3701	2.8059
∠(O2S1O3)	116.83	105.79	105.79
∠(C8S1C4)	105.57	108.80	111.85
∠(C8S1O3)	107.27	111.15	109.75
∠(H5C4H6)	111.98	111.42	108.67
∠(O23Li13)	164.32		
∠(O2Li13O3)		105.79	75.33
∠(H6Cl12H9)	55.04	69.49	62.16
∠(O2S1Cl12)	174.72	162.93	127.10
φ(Li13O3S1O2)	180.0	0	0
φ(Li13S1C4C8)	–92.5	179.1	180.0
Energy, Hartree	–1093.56823852	–1093.49717076	–1093.49534928
Dipole Moment, D	3.30	16.23	17.33

Table 3

Some optimized structural parameters for 1:1 LiCl–DESO2 stable complexes and transition state at RHF/6-311++G(d, p) level

Parameters*	LiCl–DESO2 (I structure)	LiCl–DESO2 (II structure)	LiCl–DESO2 (transition state)
r(S1–O3)	1.4619	1.4692	1.4761
r(S1–O2)	1.4301	1.4795	1.4761
r(S1–C4)	1.7829	1.7761	1.7775
r(S1–C7)	1.7829	1.7761	1.7775
r(C4–C10)	1.5272	1.5245	1.5247
r(C4–H5)	1.0837	1.0845	1.0812
r(C4–H6)	1.0834	1.0884	1.0812
r(C7–H8)	1.0834	1.0884	1.0812
r(C10–H11)	1.0838	1.0833	1.0833
r(Li19–O2)	4.2542	1.9239	1.9143
r(Li19–O)	1.8347	1.9010	1.9143
r(Li19–Cl18)	2.1148	5.9268	6.3543
r(Cl18–H8)	3.0244	2.3673	2.8004
∠(O2S1O3)	116.27	105.48	105.54
∠(C7S1C4)	104.89	107.62	110.03
∠(C4S1O3)	107.62	111.51	110.30
∠(H5C4H6)	109.62	109.41	106.22
∠(O2O3Li19)	164.82	52.59	52.13
∠(O2Li19O3)	8.70	75.69	75.75
∠(H6Cl18H8)	51.55	64.59	58.22
∠(O2S1Cl18)	173.16	164.14	127.23
φ(Li19O3S1O2)	180.0	0.0	0.0
φ(Li19S1C4C7)	–92.9	179.2	180.0
Energy, Hartree	–1171.65984234	–1171.59010234	–1171.58784999
Dipole Moment, D	3.7557	16.0661	17.5157
$\nu_{as}(\text{SO}_2)$ , $\text{cm}^{-1}$	1352 (1229)*	1246 (1133)*	1235 (1127)*
$\nu_s(\text{SO}_2)$ , $\text{cm}^{-1}$	1212 (1102)*	1203 (1094)*	1194 (1085)*

\* Scaling factor is equal to 0.909.

The main structural parameters of 1:1 LiCl–DMSO2 and 1:1 LiCl–DESO2 stable complexes optimized at the RHF/6-311++G(d, p) level of theory are presented in Tab. 2 and 3, from here it is seen that the interaction between Li ion and DMSO2 or DESO2 molecule leads to lengthening of the S–O bonds, shortening of the C–S bonds, at the same time the solvation of Cl-ion leads to lengthening of the C–H bonds involving in the interaction. The effect of interaction on the C–H bond length and H–C–H bond angles are small. On the other hand, the bond angles around the sulfur atom of the DMSO2 (or DESO2) show more significant changes. In addition, all these effects are more pronounced in the case of II structure. The results obtained indicate that in sulfone solutions the cation has more preferential solvation than anion.

The transition state structure for LiCl–DMSO2 and LiCl–DESO2 system was determined also (Fig. 2, c and Fig. 3, c). As it is well known a transition state is a first order saddle point on a potential energy surface. Thus, the second order derivative of potential energy is negative with respect to one internal coordinate at that point, and is positive with respect to all other internal coordinates. In order to confirm a transition state we have performed vibrational analysis at the same computational level as the geometry optimization.

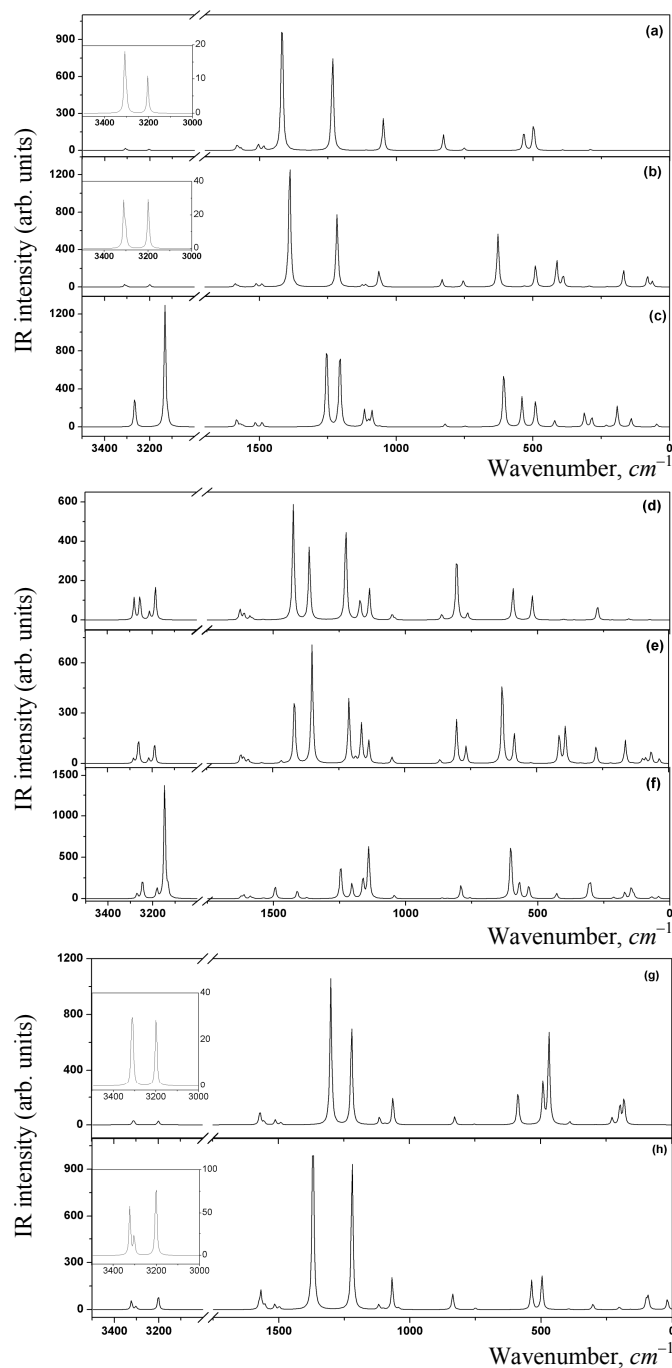


Fig. 4. Calculated (RHF/6-311++G(d, p)) IR spectra of isolated DMSO2 (a) and DESO2 (d); 1:1 LiCl-DMSO2 system: I structure (b), II structure (c); 1:1 LiCl-DESO2 system: I structure (e), II structure (f), DMSO2/Li<sup>+</sup> (g), DMSO2/Cl<sup>-</sup> (h).

The IR spectrum of this structure is characterized by one imaginary frequency at  $-23.71\text{ cm}^{-1}$  in the case of LiCl-DMSO2 and at  $-21.90\text{ cm}^{-1}$  for LiCl-DESO2. It should be noted, that the normal mode corresponding to this

imaginary frequency represents the chlorine-ion migration. The energy difference between the II structure and transition state is  $4.8 \text{ kJ/mol}$  for LiCl–DMSO<sub>2</sub> and  $5.9 \text{ kJ/mol}$  for LiCl–DESO<sub>2</sub>. Besides the calculated interaction energy between LiCl and DESO<sub>2</sub> molecules in the I structure is more by  $0.44 \text{ kJ/mol}$ , in the II structure is more by  $3.9 \text{ kJ/mol}$  in comparison with DMSO<sub>2</sub>.

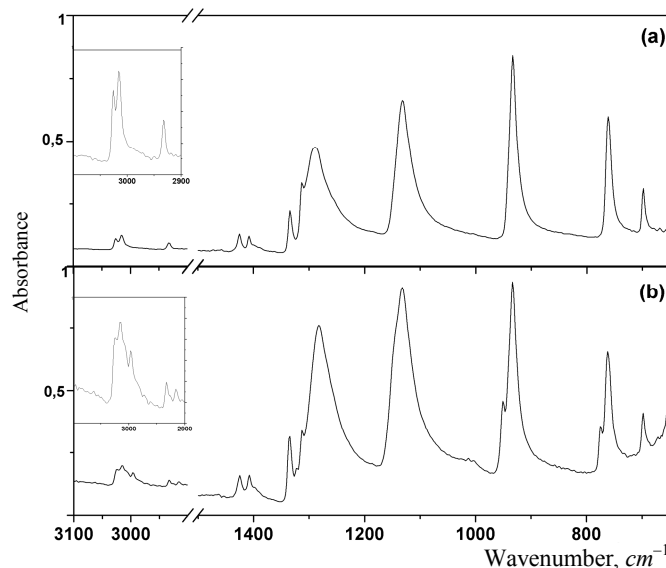


Fig. 5. ATR FT IR spectra of solid crystalline DMSO<sub>2</sub> (a) 1:4 LiCl–DMSO<sub>2</sub> solid solution (b).

The calculated vibrational frequencies of fundamental modes of free DMSO<sub>2</sub> are listed in Tab. 3 and compared there to those of the 1:1 LiCl–DMSO<sub>2</sub> system. The theoretical IR spectra of isolated DMSO<sub>2</sub>, DESO<sub>2</sub> molecules, as well as 1:1 LiCl–DMSO<sub>2</sub> and 1:1 LiCl–DESO<sub>2</sub> systems are presented in Fig. 4. Besides that the comparison of calculated spectra with the experimental spectra of solid DMSO<sub>2</sub> and 1:4 LiCl–DMSO<sub>2</sub> solution shown in Fig. 5 has been done.

It is well known that the calculated RHF or “unscaled” harmonic frequencies could significantly overestimate experimental values due to lack of electron correlation, insufficient basis sets and anharmonicity. The appropriate scaling factor for RHF/6-311++G(d, p) level of theory (equal 0.909) was used to obtain an agreement between observed and calculated wavenumbers. A little difference in frequencies between the calculation and the experiment can be considered due to the different states of matter. It should be noted, that in the present case theoretical calculations belong to gaseous state of isolated molecules and the experimental spectra belong to the solid state. Usually, the vibration frequencies in the gas state are larger than in the condensed state.

C–H stretching vibrations of sulfones are observed within the region 3100–2900  $\text{cm}^{-1}$ . In the FTIR spectrum of solid DMSO<sub>2</sub> three medium bands at 3026, 3015 and 2932  $\text{cm}^{-1}$  are assigned to the C–H stretching vibrations. This result is consistent with literature data [15, 16]. In the presence of LiCl in the C–H stretching region the peaks at 3026, 3015 and 2933  $\text{cm}^{-1}$  are observed as before, additionally new peaks at 3009, 2997 and 2915  $\text{cm}^{-1}$  appeared in experimental spectrum, which are attributed to the solvated species.

Table 4

*IR vibrational frequencies of DMSO2 and LiCl–DMSO2 systems and their assignments*

	DMSO <sub>2</sub> , $\nu$ , $cm^{-1}$	1:1 LiCl–DMSO <sub>2</sub> I structure, $\nu$ , $cm^{-1}$		1:1 LiCl–DMSO <sub>2</sub> II structure, $\nu$ , $cm^{-1}$	
Assignment	unscaled (scaled*)	unscaled (scaled)	assignment	unscaled (scaled)	assignment
$\nu_{as}(CH_3)$	3309 (3008) vw	3312(3010) w	$\nu_{as}(CH_3)$	3306 (3005) vw	$\nu_{as}(CH_3)$
$\nu_{as}(CH_3)$	3304 (3003)	3307 (3006) vvw	$\nu_{as}(CH_3)$	3303 (3002) vw	$\nu_{as}(CH_3)$
$\nu_{as}(CH_3)$	3301 (3001) vw	3302 (3002) vvw	$\nu_{as}(CH_3)$	3266 (2969) m	$\nu_{as}(CH_3)$
$\nu_{as}(CH_3)$	3300 (2999) vvw	3300 (3000) vvw	$\nu_{as}(CH_3)$	3262 (2965) w	$\nu_{as}(CH_3)$
$\nu_s(CH_3)$	3204 (2912) vw	3199 (2908) w	$\nu_s(CH_3)$	3132 (2847) vs	$\nu_s(CH_3)$
$\nu_s(CH_3)$	3200 (2909) vvw	3196 (2905) vvw	$\nu_s(CH_3)$	3119 (2835) vw	$\nu_s(CH_3)$
$\delta(CH_3)$	1583 (1439) w	1588 (1444) w	$\delta(CH_3)$	1583 (1439) w	$\delta(CH_3)$
$\delta(CH_3)$	1577 (1433) vw	1580 (1436) vw	$\delta(CH_3)$	1570 (1427) vw	$\delta(CH_3)$
$\delta(CH_3)$	1568 (1425)	1577 (1433) vw	$\delta(CH_3)$	1560 (1418) vw	$\delta(CH_3)$
$\delta(CH_3)$	1568 (1425) vw	1565 (1422) vvw	$\delta(CH_3)$	1539 (1399) vvw	$\delta(CH_3)$
$\delta(CH_3)$	1505 (1368) w	1511(1374) w	$\delta(CH_3)$	1514 (1377) vw	$\delta(CH_3)$
$\delta(CH_3)$	1485 (1350) w	1491(1355) w	$\delta(CH_3)$	1490 (1355) vw	$\delta(CH_3)$
$\nu_{as}(SO_2)$	1418 (1289) vs	1389 (1263) vs	$\nu_{as}(SO_2)$	1254 (1140) s	$\nu_{as}(SO_2)$
$\nu_s(SO_2)$	1233 (1121) s	1216 (1106) s	$\nu_s(SO_2)$	1206 (1096) s	$\nu_s(SO_2)$
$\delta(CH_3)$	1110 (1009) vvw	1124 (1022) w	$\delta(CH_3)$	1116 (1014) m	$\delta(CH_3)$
$\delta(CH_3)$	1100 (1000) vvw	1111 (1010) w	$\delta(CH_3)$	1101(1001) w	$\delta(CH_3)$
$\delta(CH_3)$	1048 (953) m	1063 (966) m	$\delta(CH_3)$	1088 (989) m	$\delta(CH_3)$
$\delta(CH_3)$	1039 (944) w	1056 (960) w	$\delta(CH_3)$	1059 (963) vvw	$\delta(CH_3)$
$\nu_{as}(CSC)$	828 (753) m	832 (757) w	$\nu_{as}(CSC)$	821(746) vw	$\nu_{as}(CSC)$
$\nu_s(CSC)$	752 (684) w	755 686) w	$\nu_s(CSC)$	748 (679) vvw	$\nu_s(CSC)$
$\delta(OSO)$	534 (485) s–m	628 (571) vs	$\delta(OSO)$ $\delta(OLiO)$	606(551) vs	$\delta(OSO)$ $\delta(OLiO)$
	498–199 (453–181)	531–64 (483–58)		540–47 (491–43)	

\* Scaling factor is equal to 0.909, relative intensities indicate: vs – very strong; s – strong; m – medium; w – weak; vw – very weak; vvw – very very weak.

According to the calculation results the effects of complexation on the frequencies and, more noticeably, on IR intensities of C–H stretching modes in the case of I structure are minor compared to that of II structure. Particularly, as it is seen from Tab. 4, for the calculated  $\nu_{as}(CH_3)$  and  $\nu_s(CH_3)$  modes of isolated DMSO<sub>2</sub> molecule observed at 3309, 3301 and 3204  $cm^{-1}$ , there is a small change in frequencies (3312, 3302 and 3199  $cm^{-1}$ ) and intensities in the case of LiCl–DMSO<sub>2</sub> I structure (Fig. 4, a and b). However, for the LiCl–DMSO<sub>2</sub> II structure there is a very significant shift in frequencies (3306, 3266 and 3132  $cm^{-1}$ ) and a strong boost in intensities (Fig. 4, a and c), making them even stronger than S–O stretching modes according to the calculation results. Thus, the new peaks in experimental LiCl–DMSO<sub>2</sub> IR spectra can be attributed to the II structure, while for the I structure no reliable assignments can be made due to intensities and frequencies, comparable to that of pure DMSO<sub>2</sub>. It should be noted, that these new peaks have lower intensities in measured IR spectrum, than it is expected from calculation results for the II structure solely, therefore, we conclude that concentration of the II structure in LiCl–DMSO<sub>2</sub> solution is relatively small. Comparing absolute values of calculated HF energies from Tab. 2, we conclude that the I structure is favored by 186  $kJ/mol$  compared to the II structure in gas phase, thus it is the predominating species in this system.

This contrast in IR spectra of the II structure compared to the I structure, especially the pronounced effect of LiCl on intensities of C–H stretching modes, is hard to explain only on the basis of solute-solvent interaction strengths differences. For example, Li13–O3 distance in the I structure is shorter than in the II structure



(1.8413 and 1.9086 Å), indicating a stronger solvation in the I structure, however its IR spectra in the C–H stretching region is nearly unaffected compared to isolated DMSO2.

This phenomenon can be explained more conveniently, if we take into account the electrostatic field, created by  $\text{Li}^+\dots\text{Cl}^-$  ion pair, affecting the electron density distribution of sulfone molecule. In the I structure LiCl forms a close contact ion pair ( $r(\text{Li}13\text{--Cl}14)=2.12$  Å), thus compacting electrostatic field in between, therefore, the solvent molecule stays comparably unaffected. For the structure II a solvent-separated ion pair is formed, where electrostatic field lines cross through the sulfone molecule, causing a significant polarization of bonds, making C–H bonds more polar and thus more IR active (ca. 30 times stronger  $\nu_{\text{as}}(\text{CH}_3)$ ,  $\nu_{\text{s}}(\text{CH}_3)$  absorbance compared to pure DMSO2). It should be noted, that these effects are not observed in the case of DMSO2– $\text{Li}^+$  and DMSO2– $\text{Cl}^-$  systems (note low C–H intensities), which are derived from the II structure by removing one or the other counter ion (Fig. 4, g and h). Thus, the total effect cannot be explained by specific ion-solvent interactions at all. This phenomenon is most widely known as vibrational Stark effect, which was first pursued by Boxer et al. by the example of nitrile group absorption dependence in external electric fields of different strengths [17]. Nowadays it becomes a popular method for indirect measurement of electrical fields in biological systems (protein cavities), for ion-pairing structure identifications [18], etc. Similar effects were observed in LiCl–DES02 system and are explained accordingly (Fig. 4, e and f).

The characteristic bands of S–O stretching vibrations of dimethyl sulfone are observed in the region 1300–1100  $\text{cm}^{-1}$ . The strong FTIR band at 1289  $\text{cm}^{-1}$  is assigned to the S–O antisymmetric stretching vibration, and band at 1132  $\text{cm}^{-1}$  is assigned to the S–O symmetric stretching vibration. In IR spectrum of 1:4 LiCl–DMSO2 solution the S–O antisymmetric stretching vibration is slightly shifted to the low frequency region (1282  $\text{cm}^{-1}$ ), and the difference between S–O antisymmetric and symmetric stretching vibration is 155  $\text{cm}^{-1}$ . It is notable that theoretically calculated values for DMSO2 molecule after scaling are 1289 and 1121  $\text{cm}^{-1}$  respectively. It should be noted, that the calculated spectra of LiCl–DMSO2 systems and LiCl–DES02 systems for the I and II structures differ significantly from each other. While for the I structure the difference between calculated S–O antisymmetric and symmetric stretching vibration frequencies is 157  $\text{cm}^{-1}$ , which coincides with the experimental spectrum, for the II structure the difference is only 48  $\text{cm}^{-1}$ . It should be noted, however, that for the II structure calculated spectra for both S–O stretching modes are less intensive compared to the I structure (ca. 2 times, Fig. 4, b and c) and also it seems to have lower concentration, as it was discussed above, therefore, its contribution in experimental spectrum is expected to be small.

Thus, the results obtained indicate that LiCl in sulfones forms two different species: contact ion pair (I structure) and solvent-separated ion pair (II structure), which were identified and characterized by analysis of experimental and calculated IR spectra, both in CH and SO stretching regions. The difference between properties of these two structures are explained in the frame of vibrational Stark effect (i.e. the action of electric fields generated by  $\text{Li}^+\dots\text{Cl}^-$  ion pairs on the solvent molecule), rather than by specific solute-solvent interactions only.

*This work was partially supported by the RA MES SCS, in the frames of the research project N 15T-1D005.*

Received 14.11.2017

## REFERENCES

1. **Reddy T.B., Linden D.** Linden's Handbook of Batteries (4th ed.). McGraw-Hill, 2011, 1457 p.
2. **Xu K., Angell C.A.** Sulfone-Based Electrolytes for Lithium Ion Batteries. // *J. Electrochem. Soc.*, 2002, v. 149, p. A920–A926.
3. **Abouimrane A., Belharouak I., Amine K.** Sulfone-Based Electrolytes for High-Voltage Li Ion Batteries. // *Electrochem. Commun.*, 2009, v. 11, p. 1073–1076.
4. **Clark T., Murray J.S., Lane P., Politzer P.** Why are Dimethyl Sulfoxide and Dimethyl Sulfone Such Good Solvents? // *J. Mol. Model.*, 2008, v. 14, p. 689–697.
5. **Wang Y., Xing L., Li W., Bedrov D.** Why Do Sulfone-Based Electrolytes Show Stability at High Voltages? Insight from Density Functional Theory. // *J. Phys. Chem. Lett.*, 2013, v. 4, p. 3992–3999.
6. **Lee S.-Y., Ueno K., Angell C.A.** Lithium Salt Solutions in Mixed Sulfone and Sulfone-Carbonate Solvents: A Walden Plot Analysis of the Maximally Conductive Compositions. // *J. Phys. Chem.*, 2012, v. 116, p. 23915–23920.
7. **Tretyakov D., Prisiazhny V.D., Gafurov M.M., Rabadov K.S., Kirillov S.A.** Formation of Contact Ion Pairs and Solvation of  $\text{Li}^+$  Ion in Sulfones: Phase Diagrams, Conductivity, Raman Spectra and Dynamics. // *J. Chem. Eng. Data*, 2010, v. 55, № 5, p. 1958–1964.
8. **Watanabe Y., Kinoshita S.-I., Wada S., Hoshino K., Morimoto H., Tobishima S.-I.** Electrochemical Properties and Lithium Ion Solvation Behavior of Sulfone–Ester Mixed Electrolytes for High-Voltage Rechargeable Lithium Cells. // *J. Power Sources*, 2008, v. 179, p. 770–779.
9. **Yanase S., Oi T.** Solvation of Lithium Ion in Organic Electrolyte Solutions and Its Isotopic Reduced Function Ratios Studied by *ab initio* Molecular Orbital Method. // *J. Nucl. Sci. Technol.*, 2002, v. 39, № 10, p. 1060–1064.
10. Gaussian 09, Revision D.01, **Frisch M.J., Trucks G.W., Schlegel H.B., Scuseria G.E., Robb M.A., Cheeseman J.R., Scalmani G., Barone V., Mennucci B., Petersson G.A., Nakatsuji H., Caricato M., Li X., Hratchian H.P., Izmaylov A.F., Bloino J., Zheng G., Sonnenberg J.L., Hada M., Ehara M., Toyota K., Fukuda R., Hasegawa J., Ishida M., Nakajima T., Honda Y., Kitao O., Nakai H., Vreven T., Montgomery J.A.Jr., Peralta J.E., Ogliaro F., Bearpark M., Heyd J.J., Brothers E., Kudin K.N., Staroverov V.N., Keith T., Kobayashi R., Normand J., Raghavachari K., Rendell A., Burant J.C., Iyengar S.S., Tomasi J., Cossi M., Rega N., Millam J.M., Klene M., Knox J.E., Cross J.B., Bakken V., Adamo C., Jaramillo J., Gomperts R., Stratmann R.E., Yazyev O., Austin A.J., Cammi R., Pomelli C., Ochterski J.W., Martin R.L., Morokuma K., Zakrzewski V.G., Voth G.A., Salvador P., Dannenberg J.J., Dapprich S., Daniels A.D., Farkas O., Foresman J.B., Ortiz J.V., Cioslowski J., Fox D.J.** Gaussian, Inc., Wallingford CT, 2013.
11. **Frisch A., Nielson A.B., Holder A.J.** GAUSSVIEW User Manual, Gaussian Inc. Pittsburgh PA, 2000.
12. **Saito S., Makino F.** The Microwave Spectrum of Dimethyl Sulfone. // *Bull. Chem. Soc. Japan*, 1972, v. 45, p. 92–94.
13. **Buncel E., Decouzon M., Formento A., Gal J.-F., Herreros M., Li L., Pierre-Charles Mariallmar P.-Ch., Koppel I., Kurg R.** Lithium-Cation and Proton Affinities of Sulfoxides and Sulfones: A Fourier Transform Ion Cyclotron Resonance Study. // *J. Am. Soc. Mass Spectrom.*, 1997, v. 8, p. 262–269.
14. **Maxey B.W., Popov A.I.** Spectroscopic Studies of the Solvation of Alkali Metal Ions in Dialkyl Sulfoxide Solutions. // *J. Am. Chem. Soc.*, 1969, v. 91, p. 20–24.
15. **Uno T., Machida K., Hanai K.** Vibrational Spectra of Dimethyl Sulphone and Dimethyl Sulphone- $d_6$ . // *Spectrochim. Acta*, 1971, v. 27A, p. 107–118.
16. **Givan A., Grothe H., Loewenschuss A., Nielsen C.** Infrared Spectra and *ab initio* Calculations of Matrix Isolated Dimethyl Sulfone and Its Water Complex. // *Phys. Chem. Chem. Phys.*, 2002, v. 4, p. 255–263.
17. **Fried S.D., Boxer S.G.** Measuring Electric Fields and Noncovalent Interactions Using the Vibrational Stark Effect. // *Acc. Chem. Res.*, 2015, v. 48, p. 998–1006.
18. **Hack J., Grills D.C., Miller J.R., Mani T.** Identification of Ion-Pair Structures in Solution by Vibrational Stark Effects. // *J. Phys. Chem. B*, 2016, v. 120, p. 1149–1157.